

# Plasmon Modes of Axisymmetric Metallic Nanoparticles: A Group Theory Analysis

G. Gantzounis\*

*Institute of Microelectronics, NCSR “Demokritos”, GR-153 10 Athens, Greece*

*Received: August 19, 2009; Revised Manuscript Received: October 1, 2009*

We report a thorough and rigorous analysis of the plasmon modes of axisymmetric metallic nanoparticles, based on group theory techniques and block diagonalization of the scattering T matrix. In particular, we discuss plasmonic excitations under plane-wave illumination of a silver nanorod and a nanodisk, and present a detailed comparative study of elongated silver nanoparticles of different shape, but with the same length and thickness. Our methodology allows for an unambiguous classification of the eigenmodes of nonspherical particles, according to the irreducible representations of the appropriate point symmetry group, and provides a consistent explanation of relevant extinction spectra elucidating aspects of the problem to a degree that goes beyond usual interpretation.

## Introduction

The problem of scattering of electromagnetic (EM) waves by isolated particles has long been investigated in its different aspects. These investigations are motivated by a plethora of diverse applications ranging from radar meteorology<sup>1</sup> to nanomedicine.<sup>2</sup> A rigorous solution of the problem of scattering of EM waves by a homogeneous sphere of arbitrary size embedded in a homogeneous medium was given by Mie<sup>3</sup> and Debye.<sup>4</sup> On the other hand, for nonspherical scatterers, analytic solutions are only effective when the boundary surface is described conveniently in one of the coordinate systems for which the vector Helmholtz equation is separable.<sup>5–8</sup> However, because of the analytical complexity of the overall boundary value problem, even for such shapes, numerical solutions are generally more efficient<sup>9–14</sup> and are currently employed in the study of nonspherical particles of various types.

The optical properties of metallic nanoparticles attract considerable attention for a variety of reasons, not least of which are technological applications. The extinction spectrum of these particles in the visible region is characterized by pronounced resonances due to the excitation of particle plasmons.<sup>15</sup> These are collective electron oscillations at the surface of the particle that cause large enhancement of the local field and strong light absorption, effects that are interesting in nonlinear optics,<sup>16,17</sup> solar energy absorption,<sup>18,19</sup> thermal emission,<sup>20,21</sup> enhanced random lasing,<sup>22</sup> sensing and optoelectronics applications.<sup>23</sup> In particular, large scientific interest in this area is devoted to the investigation of nonspherical and core–shell particles, because of the strong tunability of their plasmon modes.<sup>24,25</sup> These particles can efficiently enhance fluorescence,<sup>26</sup> be useful in the detection of DNA hybridization,<sup>27</sup> control radiation damping,<sup>28</sup> and so forth. The most promising materials for such applications appear to be gold and silver,<sup>29–31</sup> and novel synthetic methods have led to precise control over particle size, shape, and stability.<sup>32,33</sup> Furthermore, it has been shown that a precise knowledge of the scattering cross section spectrum can give information about the particle size and shape,<sup>34</sup> and various theoretical methods have been applied for predicting and understanding the optical response of such nanoparticles.<sup>35</sup>

Although the eigenmodes of spherical particles have a well-defined multipole character and polarization (magnetic or electric) type, and can be excited by a plane wave at the resonance frequency incident from any direction and with any polarization, this is not the case with nonspherical particles. In the present article, we present a methodology, based on group theory, for a rigorous analysis of the eigenmodes of nonspherical particles. This method provides a unique framework for understanding the nature of the modes of the EM field about such a particle and their coupling efficiency with an externally incident wave (dark and bright modes). Besides single particles, the proposed methodology is also useful for the analysis of complex systems consisting of many particles. The efficiency and versatility of the various three-dimensional EM multiple-scattering methods developed in the last few decades<sup>36–45</sup> lie in the fundamental notion that the scattering properties of a composite system can be obtained from those of the individual parts comprising the system. That is to say, the optical response of an assembly is determined to a considerable extent from the properties of the individual scattering centers. Therefore, a proper rigorous analysis of the optical modes of single particles, in terms of group theory, allows for a deeper understanding of the behavior of complex structures of such particles, in the same manner as the electronic structure and resulting properties of molecules and solids can be understood from the properties of the individual atoms. Such an analysis is more or less straightforward for EM structures of spherical particles;<sup>43,46–48</sup> however, for particles of lower symmetry, the analysis is much more involved,<sup>49–51</sup> and the classification of modes as dipole, quadrupole, etc.,<sup>52</sup> is not accurate. In view of the considerable research activity relating to complex photonic architectures with building units of nonspherical shape, especially in relation to plasmonic nanostructures<sup>53–55</sup> but also in relation to optical metamaterials,<sup>56–58</sup> we believe that the present work is timely and, hopefully, useful.

The structure of this paper is as follows. In the first section we describe the scattering of EM waves by a single particle and introduce the T matrix. In the second section we discuss the symmetry of the eigenmodes of nonspherical particles. We project both vector spherical waves and plane waves to the  $C_{\infty v}$  and  $D_{\infty h}$  point groups, which are appropriate for axisymmetric particles, and discuss the condition that must be fulfilled so that

\* E-mail: ggantzou@phys.uoa.gr.

a specific mode can be excited by an incoming plane wave. In the third section we apply the above methodology to silver nanoparticles of various shapes: disks versus rods, as well as cylinders, capped cylinders, and prolate spheroids. We thoroughly analyze the corresponding extinction spectra and discuss similarities and differences in the optical response of the different shapes. Finally, a summary of all findings is given in the fourth section.

### Scattering by a Single Particle

The electric field associated with a harmonic, monochromatic EM wave, of angular frequency  $\omega$ , has the form  $\mathbf{E}(\mathbf{r}, t) = \text{Re}[\mathbf{E}(\mathbf{r}) \exp(-i\omega t)]$ . For a plane wave of wavevector  $q$ , propagating in a homogeneous medium characterized by a relative dielectric function  $\varepsilon$  and a relative magnetic permeability  $\mu$  (we shall denote it by an index 0), we have

$$\mathbf{E}_0(\mathbf{r}) = \hat{\mathbf{p}}E_0(\mathbf{q}) \exp(i\mathbf{q} \cdot \mathbf{r}) \quad (1)$$

where  $E_0$  is the magnitude and  $\hat{\mathbf{p}}$ , a unit vector, is the polarization of the electric field. The plane wave given by eq 1 can be expanded into regular vector spherical waves about a given origin of coordinates as follows:<sup>45</sup>

$$\mathbf{E}_0(\mathbf{r}) = \sum_{P=1,2} \sum_{l=1}^{\infty} \sum_{m=-l}^l a_{Plm}^0 \mathbf{J}_{Plm}(\mathbf{r}) \quad (2)$$

where  $P = 1$  or  $2$  is the polarization mode: magnetic or electric type, respectively, and  $q = \omega(\varepsilon\mu)^{1/2}/c$ , with  $c$  being the velocity of light in vacuum, is the wavenumber. The wave functions  $\mathbf{J}_{Plm}(\mathbf{r})$  are defined as

$$\begin{aligned} \mathbf{J}_{1lm}(\mathbf{r}) &= j_l(qr) \mathbf{X}_{lm}(\hat{\mathbf{r}}) \\ \mathbf{J}_{2lm}(\mathbf{r}) &= \frac{i}{q} \nabla \times \mathbf{J}_{1lm}(\mathbf{r}) \end{aligned} \quad (3)$$

with  $j_l(qr)$  being the spherical Bessel functions, which are finite everywhere, and  $\mathbf{X}_{lm}(\hat{\mathbf{r}}) \equiv -i\mathbf{r} \times \nabla Y_{lm}(\mathbf{r})$  being the vector spherical harmonics.<sup>59</sup> Finally, the expansion coefficients  $a_{Plm}^0$  can be written as

$$a_{Plm}^0 = \mathbf{A}_{Plm}^0(\hat{\mathbf{q}}) \cdot \hat{\mathbf{p}} E_0(\mathbf{q}) \quad (4)$$

with

$$\begin{aligned} \mathbf{A}_{1lm}^0(\hat{\mathbf{q}}) &= \frac{4\pi i^l (-1)^{m+1}}{\sqrt{l(l+1)}} \{ [\alpha_l^m \cos \theta e^{i\phi} Y_{l-m-1}(\theta, \phi) + \\ & m \sin \theta Y_{l-m}(\theta, \phi) + \alpha_l^{-m} \cos \theta e^{-i\phi} Y_{l-m+1}(\theta, \phi)] \hat{\mathbf{e}}_1 + \\ & i[\alpha_l^m e^{i\phi} Y_{l-m-1}(\theta, \phi) - \alpha_l^{-m} e^{-i\phi} Y_{l-m+1}(\theta, \phi)] \hat{\mathbf{e}}_2 \} \end{aligned} \quad (5)$$

and

$$\begin{aligned} \mathbf{A}_{2lm}^0(\hat{\mathbf{q}}) &= \frac{4\pi i^l (-1)^{m+1}}{\sqrt{l(l+1)}} \{ i[\alpha_l^m e^{i\phi} Y_{l-m-1}(\theta, \phi) - \\ & \alpha_l^{-m} e^{-i\phi} Y_{l-m+1}(\theta, \phi)] \hat{\mathbf{e}}_1 - [\alpha_l^m \cos \theta e^{i\phi} Y_{l-m-1}(\theta, \phi) + \\ & m \sin \theta Y_{l-m}(\theta, \phi) + \alpha_l^{-m} \cos \theta e^{-i\phi} Y_{l-m+1}(\theta, \phi)] \hat{\mathbf{e}}_2 \} \end{aligned} \quad (6)$$

where  $\alpha_l^m = (1/2)[(l-m)(l+m+1)]^{1/2}$ ;  $(\theta, \phi) \equiv \hat{\mathbf{q}}$  denotes the angular variables of  $\mathbf{q}$  in the chosen system of spherical coordinates; and  $\hat{\mathbf{e}}_1$  and  $\hat{\mathbf{e}}_2$  are the polar and azimuthal unit vectors, respectively, which are perpendicular to  $\mathbf{q}$ . We note that if  $\hat{\mathbf{p}} = \hat{\mathbf{e}}_1$  ( $\hat{\mathbf{e}}_2$ ) the wave is  $p$  ( $s$ ) polarized.

We now consider a homogeneous particle of arbitrary shape, centered at the origin of coordinates, and assume that its relative dielectric function  $\varepsilon_s$  and/or magnetic permeability  $\mu_s$ , in general complex functions of  $\omega$ , are different from those of the surrounding medium. When the plane wave described by eq 2 is incident on the particle, it is scattered by it, so that the wave field outside the particle consists of the incident wave and a scattered wave, which can be expanded in spherical waves as follows:

$$\mathbf{E}_{\text{sc}}(\mathbf{r}) = \sum_{Plm} a_{Plm}^+ \mathbf{H}_{Plm}(\mathbf{q}\mathbf{r}) \quad (7)$$

where  $\mathbf{H}_{1lm}(\mathbf{q}\mathbf{r}) = h_l^+(qr) \mathbf{X}_{lm}(\hat{\mathbf{r}})$  and  $\mathbf{H}_{2lm}(\mathbf{q}\mathbf{r}) = (iq) \nabla \times \mathbf{H}_{1lm}(\mathbf{q}\mathbf{r})$ , with  $h_l^+(qr)$  being the spherical Hankel functions appropriate to outgoing spherical waves:  $h_l^+(qr) \approx (-i)^l \exp(iqr)/iqr$  as  $r \rightarrow \infty$ .

In general, the expansion coefficients  $a_{Plm}^+$  of the scattered wave can be expressed in terms of those of the incident wave ( $a_{Plm}^0$ ) through the scattering T matrix as follows:

$$a_{Plm}^+ = \sum_{P'l'm'} T_{Plm;P'l'm'} a_{P'l'm'}^0 \quad (8)$$

The T matrix is evaluated, through different methods, by imposing the proper boundary conditions, i.e., continuity of the EM field at the surface of the particle, and describes the EM response of the particle. For example, the scattering and extinction cross sections are given by<sup>45</sup>

$$\begin{aligned} \sigma_{\text{sc}} &= \frac{1}{q^2} \sum_{Plm} \left| \sum_{P'l'm'} T_{Plm;P'l'm'} \mathbf{A}_{P'l'm'}^0 \cdot \hat{\mathbf{p}} \right|^2 \\ \sigma_{\text{ext}} &= -\frac{1}{q^2} \text{Re} \sum_{Plm} (\mathbf{A}_{Plm}^0 \cdot \hat{\mathbf{p}})^* \sum_{P'l'm'} T_{Plm;P'l'm'} \mathbf{A}_{P'l'm'}^0 \cdot \hat{\mathbf{p}} \end{aligned} \quad (9)$$

respectively, where  $*$  denotes a complex conjugate, while the absorption cross section is defined by  $\sigma_{\text{abs}} = \sigma_{\text{ext}} - \sigma_{\text{sc}}$ . It is clear from eq 9 that, in general, the cross sections depend on the polarization and the direction of propagation of the incident wave. In the particular case of a spherically symmetric particle, the T matrix becomes diagonal:  $T_{Plm;P'l'm'} = T_{Pl} \delta_{PP'} \delta_{ll'} \delta_{mm'}$ , and the cross sections depend only on the T matrix, since  $\sum_m \mathbf{A}_{Plm}^0 \cdot \hat{\mathbf{p}}^2 = 2\pi(2l+1)$ . The particle eigenmodes, i.e., wave field solutions in the absence of incoming wave, are obtained through the condition  $\det \mathbf{T}^{-1} = 0$ , which follows from eq 8. In general, a single particle supports resonant modes of the EM field at the poles of the eigenvalues of the corresponding T matrix in the lower complex frequency half-plane, as requested by the causality condition, near the real axis, i.e., at  $\omega_i - i\gamma_i$ ,  $\gamma_i \geq 0$ ;  $\omega_i$  is the eigenfrequency, while  $\gamma_i$  denotes the inverse of the lifetime of the respective mode. Contrary to the case of spherical scatterers, the T matrix of a nonspherical particle is not diagonal in the spherical-wave basis, and thus no unambiguous classification of its eigenvalues, according to polarization and angular momentum, can be made. Though the plasmon modes of nonspherical nanoparticles may also have a predominant

polarization and  $2^l$ -pole character,<sup>61</sup> a rigorous assignment of the different modes can be made by using group theory.<sup>51,62</sup>

### Symmetry of Particle Eigenmodes

The symmetry transformations that leave a given particle invariant form a subgroup of the orthogonal point group  $O(3)$ . Such symmetry operations are the identity ( $E$ ), the inversion ( $I$ ), rotations through an angle  $2\pi/n$  around an axis  $A$  ( $C_{nA}$ ), as well as combinations of them, and transform a scalar ( $f$ ) or vector ( $\mathbf{F}$ ) function as follows:<sup>64</sup>

$$\begin{aligned} Rf(\mathbf{r}) &= f(\mathbf{R}^{-1}\mathbf{r}) \quad \text{or} \\ \mathbf{RF}(\mathbf{r}) &= \mathbf{RF}(\mathbf{R}^{-1}\mathbf{r}) \end{aligned} \quad (10)$$

respectively, where  $\mathbf{R}$  is the transformation matrix in the three-dimensional euclidian space, which corresponds to operation  $R$ . Let us consider application of proper ( $R$ ) and improper ( $IR$ ) rotations to the vector spherical waves. It is well-known that, while the polar vector operators commute with  $R$ , i.e.,  $\mathbf{R}\mathbf{r} = \mathbf{r}\mathbf{R}$ , or  $R\mathbf{V} = \mathbf{V}R$ , their vector product transforms like a pseudovector, i.e.,  $R(\mathbf{r} \times \mathbf{V}) = \det[\mathbf{R}](\mathbf{r} \times \mathbf{V})R$ .<sup>65</sup> As a result, a vector spherical wave of electric type,  $\mathbf{F}_{2lm}(\mathbf{r})$  ( $\mathbf{F} = \mathbf{J}$  or  $\mathbf{H}$ ), which can be written in the form  $[f_1(\mathbf{r})\mathbf{r} + f_2(\mathbf{r})\nabla]Y_{lm}(\hat{\mathbf{r}})$ , is always transformed like  $Y_{lm}(\hat{\mathbf{r}})$ , i.e., as a scalar spherical wave. On the contrary, a vector spherical wave of magnetic type,  $\mathbf{F}_{1lm}(\mathbf{r})$  ( $\mathbf{F} = \mathbf{J}$  or  $\mathbf{H}$ ), which can be written in the form  $f(\mathbf{r})(\mathbf{r} \times \nabla)Y_{lm}(\hat{\mathbf{r}})$ , is transformed like  $Y_{lm}(\hat{\mathbf{r}})$  for proper rotations and with an opposite sign for improper rotations.

We shall now project the vector spherical waves  $\mathbf{F}_{Plm}(\mathbf{r})$ , following the above rules (see also the Supporting Information), onto the irreducible representations of the  $C_{\infty v}$  and  $D_{\infty h}$  point groups, which are appropriate for axisymmetric particles and axisymmetric particles with an additional mirror plane normal to the symmetry axis (cylindrical symmetry), respectively. For the  $C_{\infty v}$  group we obtain

$$\begin{aligned} \mathcal{P}^{(A_1)}\mathbf{F}_{Plm}(\mathbf{r}) &= \delta_{m0} \frac{[1 + (-1)^P]}{2} \mathbf{F}_{Plm}(\mathbf{r}) \\ \mathcal{P}^{(A_2)}\mathbf{F}_{Plm}(\mathbf{r}) &= \delta_{m0} \frac{[1 - (-1)^P]}{2} \mathbf{F}_{Plm}(\mathbf{r}) \\ \mathcal{P}^{(E_n)}\mathbf{F}_{Plm}(\mathbf{r}) &= \delta_{|mln|} \mathbf{F}_{Plm}(\mathbf{r}) \end{aligned} \quad (11)$$

i.e.,  $\{\mathbf{F}_{2l0}(\mathbf{r})\}$  and  $\{\mathbf{F}_{1l0}(\mathbf{r})\}$ , project on the one-dimensional representations  $A_1$  and  $A_2$ , respectively, while  $\{\mathbf{F}_{Plm}(\mathbf{r})\}$  projects on the two-dimensional representations  $E_{lm}$ . Similarly, for the  $D_{\infty h}$  group we obtain

$$\begin{aligned} \mathcal{P}^{(A_{1g})}\mathbf{F}_{Plm}(\mathbf{r}) &= \delta_{m0} \frac{[1 + (-1)^P][1 + (-1)^l]}{4} \mathbf{F}_{Plm}(\mathbf{r}) \\ \mathcal{P}^{(A_{1u})}\mathbf{F}_{Plm}(\mathbf{r}) &= \delta_{m0} \frac{[1 - (-1)^P][1 + (-1)^l]}{4} \mathbf{F}_{Plm}(\mathbf{r}) \\ \mathcal{P}^{(A_{2g})}\mathbf{F}_{Plm}(\mathbf{r}) &= \delta_{m0} \frac{[1 - (-1)^P][1 - (-1)^l]}{4} \mathbf{F}_{Plm}(\mathbf{r}) \\ \mathcal{P}^{(A_{2u})}\mathbf{F}_{Plm}(\mathbf{r}) &= \delta_{m0} \frac{[1 + (-1)^P][1 - (-1)^l]}{4} \mathbf{F}_{Plm}(\mathbf{r}) \\ \mathcal{P}^{(E_{ng})}\mathbf{F}_{Plm}(\mathbf{r}) &= \delta_{|mln|} \frac{1 + (-1)^{P+l}}{2} \mathbf{F}_{Plm}(\mathbf{r}) \\ \mathcal{P}^{(E_{nu})}\mathbf{F}_{Plm}(\mathbf{r}) &= \delta_{|mln|} \frac{[1 - (-1)^{P+l}]}{2} \mathbf{F}_{Plm}(\mathbf{r}) \end{aligned} \quad (12)$$

**TABLE 1: Projection of a Plane EM Wave Propagating at an Angle  $\theta$  with Respect to the  $z$  Axis, of  $s$  or  $p$  Polarization, to the Irreducible Representations of  $C_{\infty v}$  and  $D_{\infty h}$**

angle of incidence	polarization	$C_{\infty v}$	$D_{\infty h}$
$\theta = 0, \pi$	$s$ or $p$	$E_1$	$E_{1g}, E_{1u}$
$\theta \neq 0, \pi/2, \pi$	$s$	$A_2, E_n$	$A_{1u}, A_{2g}, E_{1g}, E_{1u}, E_{2g}, E_{2u}, \dots$
	$p$	$A_1, E_n$	$A_{1g}, A_{2u}, E_{1g}, E_{1u}, E_{2g}, E_{2u}, \dots$
$\theta = \pi/2$	$s$	$A_2, E_n$	$A_{2g}, E_{1u}, E_{2g}, E_{3u}, E_{4g}, \dots$
	$p$	$A_1, E_n$	$A_{2u}, E_{1g}, E_{2u}, E_{3g}, E_{4u}, \dots$

i.e.,  $\{\mathbf{F}_{2l0}(\mathbf{r}), l:\text{even}\}$ ,  $\{\mathbf{F}_{1l0}(\mathbf{r}), l:\text{even}\}$ ,  $\{\mathbf{F}_{1l0}(\mathbf{r}), l:\text{odd}\}$ , and  $\{\mathbf{F}_{2l0}(\mathbf{r}), l:\text{odd}\}$  project on the one-dimensional representations  $A_{1g}$ ,  $A_{1u}$ ,  $A_{2g}$ , and  $A_{2u}$ , respectively, while  $\{\mathbf{F}_{Plm}(\mathbf{r}), P + l:\text{even}\}$  and  $\{\mathbf{F}_{Plm}(\mathbf{r}), P + l:\text{odd}\}$  project on the two-dimensional representations  $E_{lmg}$  and  $E_{lmu}$ , respectively.

In order to excite an eigenmode of specific symmetry, compatibility with the symmetry of the incident field is necessary, i.e., the corresponding coefficients  $a_{Plm}^0$  of eq 2 must be nonzero. For incidence along the particle axis ( $\theta = 0, \pi$ ), from eqs 5 and 6 we find that  $|\mathbf{A}_{Plm}^0 \cdot \hat{\mathbf{p}}|^2 = (2l + 1)\pi\delta_{ml1}$ , i.e., both  $s$ - and  $p$ -polarized waves can excite states only of  $E_1$  symmetry in the case of the  $C_{\infty v}$  group, or of  $E_{1g}$  and  $E_{1u}$  symmetry in the case of the  $D_{\infty h}$  group. If  $\theta = \pi/2$ ,  $|\mathbf{A}_{Plm}^0 \cdot \hat{\mathbf{p}}|^2 \neq 0$  if and only if  $l + m + P$  is even (odd) for  $s$ - ( $p$ -) polarized waves. At any other angle of incidence ( $\theta \neq 0, \pi/2, \pi$ ) all doubly degenerate modes can be excited. Furthermore,  $\mathbf{A}_{l0}^0 \cdot \hat{\mathbf{e}}_1 = \mathbf{A}_{2l0}^0 \cdot \hat{\mathbf{e}}_2 = 0$  and  $\mathbf{A}_{1l0}^0 \cdot \hat{\mathbf{e}}_2 = \mathbf{A}_{2l0}^0 \cdot \hat{\mathbf{e}}_1 = 4\pi^{l/2} Y_{l1}(\theta, 0)$ . Therefore, a  $p$ -polarized wave for  $\theta \neq 0, \pi/2$ , and  $\pi$  can excite, in addition, nondegenerate modes of  $A_1$  symmetry in the case of the  $C_{\infty v}$  group or of  $A_{1g}$  and  $A_{2u}$  symmetry in the case of the  $D_{\infty h}$  group. Correspondingly, an  $s$ -polarized wave for  $\theta \neq 0, \pi/2$ , and  $\pi$  can excite nondegenerate modes of  $A_2$  symmetry in the case of the  $C_{\infty v}$  group or of  $A_{1u}$  and  $A_{2g}$  symmetry in the case of the  $D_{\infty h}$  group. These results are summarized in Table 1.

In the specific case of axisymmetric particles, i.e., particles that are invariant under the symmetry operations of the  $C_{\infty v}$  group, the evaluation of the eigenvalues and eigenvectors of  $\mathbf{T}$  is simplified by taking advantage of its block-diagonal form  $T_{Plm; P'l'm'} = T_{Pl; P'l}^m \delta_{mm'}$ . For  $m \neq 0$ , since  $T_{Pl; P'l}^{-m} = (-1)^{P+P'} T_{Pl; P'l}^m$ , the two submatrices  $\mathbf{T}^{\pm ml}$  have the same set of eigenvalues, as follows from basic matrix algebra for partitioned matrices,<sup>63</sup> while for  $m = 0$ ,  $T_{Pl; P'l}^0 = T_{Pl}^{00} \delta_{PP'}$ .<sup>12</sup> If we further assume cylindrical symmetry, i.e., particles that are invariant under the symmetry operations of the  $D_{\infty h}$  group, the individual  $\mathbf{T}^m$  also take a block-diagonal form: Their elements are identically zero, unless  $P + l$  and  $P' + l'$  have the same parity, even or odd, these blocks corresponding to the two-dimensional irreducible representations  $E_{lmg}$  or  $E_{lmu}$  of  $D_{\infty h}$ , respectively. For  $m = 0$ ,  $T_{Pl; P'l}^0 = T_{Pl}^{00} \delta_{PP'}$ , where  $T_{Pl}^{00} = 0$  if  $l$  and  $l'$  do not have the same parity. In this case, according to the previous discussion, the submatrices correspond to the one-dimensional irreducible representations:  $A_{1g}$  for  $l, l':\text{even}$  and  $P = 2$ ;  $A_{2u}$  for  $l, l':\text{even}$  and  $P = 1$ ;  $A_{2g}$  for  $l, l':\text{odd}$  and  $P = 1$ ;  $A_{1u}$  for  $l, l':\text{odd}$  and  $P = 2$ . A given mode can be excited only if the electric field component of the incident light has a nonvanishing projection onto the appropriate irreducible subspace. For example, as discussed in the previous paragraph, a plane EM wave incident at an angle  $\theta$  ( $0 < \theta < \pi/2$ ) with respect to the particle axis (taken as the  $z$  axis) can excite modes of  $A_{1u}$ ,  $A_{2g}$ ,  $E_{lmg}$ ,  $E_{lmu} \forall m$  symmetry if it is polarized normally to the particle axis ( $s$  polarization) and modes of  $A_{1g}$ ,  $A_{2u}$ ,  $E_{lmg}$ ,  $E_{lmu} \forall m$  symmetry if it is polarized in the plane of incidence defined by the direction of incidence and the particle axis ( $p$  polarization). The different

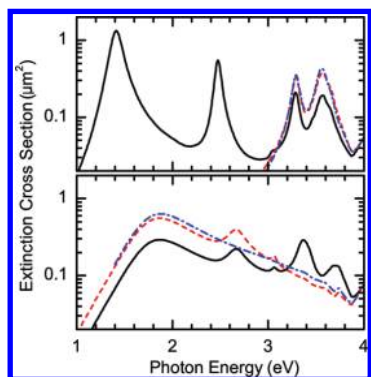


**Figure 1.** Extinction cross section of cylindrical silver nanoparticles in air, for  $p$ - (solid line) and  $s$ - (dashed line) polarized light incident at an angle  $\theta = \pi/4$  with respect to the particle axis. The results for  $\theta = 0$  (dash-dotted line) are also displayed. Upper diagram: Nanorods with diameter  $D = 40$  nm and length  $L = 200$  nm. Lower diagram: Nanodisks with diameter  $D = 200$  nm and thickness  $H = 40$  nm.

blocks of each  $\mathbf{T}^m$  submatrix can be readily diagonalized using standard eigenvalue–eigenvector routines for nonhermitian matrices, and thus the symmetry of the different modes is unambiguously defined from the corresponding block. Moreover, the predominant polarization and multipole character of a given mode is deduced from the form of the corresponding eigenvector.

### Applications

We shall now apply the group-theory methodology discussed in the previous section to analyze the plasmon modes of silver nanoparticles of  $D_{\infty h}$  symmetry, in air ( $\epsilon = 1$ ). We calculate the T matrix using a very efficient extended-boundary-condition (EBC) method,<sup>12</sup> properly modified.<sup>45</sup> Truncating the relevant angular-momentum expansions at  $l_{\max} = 6$ ,  $l_{\text{cut}} = 18$  and using a Gaussian quadrature integration formula with 4000 points for the integrals involved is sufficient to obtain well-converged results in all the cases considered. For the dielectric function of silver, we interpolate to the bulk values measured by Johnson and Christy<sup>66</sup> that include dissipative losses. Since absorption smooths out sharp resonance structures, we shall restrict our discussion only to modes that give discernible features in the extinction spectrum.

Figure 1 displays the extinction cross section of single silver nanocylinders in air. The upper diagram refers to a nanorod with diameter  $D = 40$  nm and length  $L = 200$  nm. In this case, the first three modes at 1.41, 2.47, and 3.04 eV of  $A_{2u}$ ,  $A_{1g}$  and  $A_{2u}$  symmetry, respectively, can be excited only by a  $p$ -polarized wave (solid line) for  $\theta \neq 0, \pi/2, \pi$  (see Table 1). The third mode appears as a shoulder because it has a relatively long lifetime and is wiped out by absorption. These  $A_{2u}$  and  $A_{1g}$  modes are mainly of electric dipole and electric quadrupole character, respectively. In the simple case of the  $A_{2u}$  eigenmodes, which are mainly of electric dipole character, the electric field oscillates along the cylinder axis. This explains why, if the electric field of the incident wave oscillates normal to the cylinder axis, it cannot couple to these modes. However, such a qualitative picture is unable to explain the selective excitation of other, more complex, modes. The peak at 3.29 eV is formed from the excitation of two doubly degenerate modes of  $E_{1g}$  and  $E_{1u}$  symmetry and thus, in agreement with Table 1, it appears for both  $s$ - and  $p$ -polarized waves incident at  $\theta = \pi/4$ , as well as for  $\theta = 0$ , as shown in Figure 1. Similarly, the peak at 3.57 eV is a double peak formed from an  $E_{1g}$  mode at 3.56 eV and an  $E_{2u}$  mode at 3.58 eV.

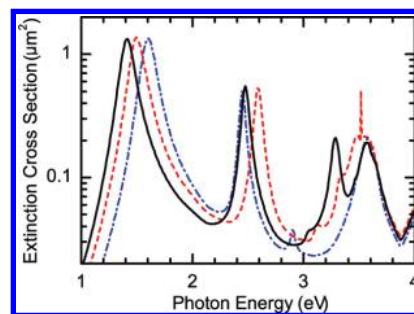


**Figure 2.** Extinction cross section of silver nanoparticles in air, for  $p$ -polarized light incident at an angle  $\theta = \pi/4$  with respect to the particle axis. The solid, dashed, and dash-dotted lines correspond to a cylinder of diameter  $D = 40$  nm and length  $L = 200$  nm, a cylinder with hemispherical caps of diameter  $D = 40$  nm and total length  $L = 200$  nm, and a prolate spheroid with major axis (axis of revolution) 200 nm long and minor axis 40 nm long, respectively.

In the lower diagram of Figure 1 we show the extinction spectrum of a silver nanodisk with diameter  $D = 200$  nm and thickness  $H = 40$  nm. The first three peaks at 1.86, 2.66, and 3.06 eV correspond to modes of  $E_{1u}$ ,  $E_{2g}$  and  $E_{3u}$  symmetry, respectively, and thus for  $\theta = 0$ , only the lowest  $E_{1u}$  mode is excited (see Table 1). The peaks at 3.36 and 3.70 eV have a similar character: They are formed mainly from two modes of  $A_{1g}$  and  $A_{2u}$  symmetry with relatively short lifetimes but also contain modes of  $E_{1g}$  symmetry, which have a mixed electric quadrupole/electric 16-pole character. The one at 3.36 eV has a relatively long lifetime, while that at 3.70 eV has a shorter lifetime. Therefore the first peak is discernible only for  $\theta = \pi/4$  and  $p$ -polarized light, because in the other cases it is completely wiped out by absorption. On the contrary, the peak at 3.70 eV subsists, even as a small structure, in all cases considered. It is worth noting that a  $p$ -polarized wave for  $\theta \neq 0, \pi/2, \pi$  can excite all the modes of the particles under consideration, and thus it can be used to probe the different modes.

In Figure 2 we compare the extinction spectra of three elongated particles with different shape but the same length ( $L = 200$  nm) and thickness ( $D = 40$  nm). A  $p$ -polarized plane wave is incident at an angle  $\theta = \pi/4$  with respect to the particle axis. The solid line corresponds to a cylinder, the dashed line corresponds to a cylinder with hemispherical caps, and the dash-dotted line corresponds to a prolate spheroid. The first two peaks at about 1.5 and 2.5 eV, of  $A_{2u}$  (mainly electric dipole character) and  $A_{1g}$  (mainly electric quadrupole character) symmetry, respectively, do not appear at the same frequency for the different nanoparticles. The third small peak of the spheroid at 2.90 eV, of  $A_{2u}$  symmetry, has a mainly electric octapole character and corresponds to the shoulder at 3.04 eV in the case of the cylinder, although its character is changed to a mixed electric dipole/electric octapole type, and to the small peak at 3.11 eV in the case of the capped cylinder, although its character becomes mainly electric dipole. In the case of the cylinder, there are two doubly degenerate modes of  $E_{1g}$  and  $E_{1u}$  symmetry at about 3.29 eV, which give a prominent peak in the extinction spectrum that is absent in the other two cases. In the same frequency region, the capped cylinder has an  $A_{1g}$  mode at 3.33 eV, which manifests itself as a small shoulder. A common feature for the three particles is the peak at 3.57 eV. This peak results from the excitation of two modes of  $E_{1g}$  and  $E_{1u}$  symmetry, at 3.56 and 3.58 eV in the case of the cylinder and at 3.57 and 3.56 eV in the case of the spheroid, respectively, while in the case of the capped cylinder only an  $E_{1u}$  mode exists at 3.58 eV. The “missing”  $E_{1g}$  mode of the capped cylinder is

shifted down to 3.48 eV and gives a peak near the sharp resonance at 3.52 eV that corresponds to a mode of  $A_{1g}$  symmetry.

The computational efficiency and reliability of the EBC T-matrix method, which was employed in the present work, has also been demonstrated through comparison with the well-established discrete dipole approximation (DDA) method. For example, significant improvement between calculations and measurements in the short-wavelength part of the extinction spectrum of randomly oriented gold nanorods has been achieved by the EBC T-matrix method, as compared with DDA simulations.<sup>52,60</sup> It is also worth noting that the DDA algorithm does not include an explicit multipole representation; instead, it considers a dense array of interacting elementary dipoles that describe the electrodynamic properties of the actual particle.<sup>67,68</sup> Therefore, an analysis of the particle eigenmodes, such as that presented here, is not straightforward.

## Conclusions

In summary, in this article we present a rigorous methodology for the analysis of the EM field eigenmodes of nonspherical particles and derive specific selection rules for coupling of these modes with an externally incident plane wave, of given polarization and propagation direction. The method, which is based on group theory and block diagonalization of the scattering T matrix, is applied to different nanoparticles of cylindrical symmetry. More specifically, we discuss in detail the plasmonic excitations of a silver nanorod and a nanodisk, and report a comprehensive comparative analysis of the plasmon modes of three different elongated silver nanoparticles: a cylinder, a capped cylinder, and a spheroid, with the same length and thickness. Our method provides a consistent interpretation of relevant extinction spectra and clarifies aspects of the problem which may be obscured with approximate treatments based on the assumption of modes with a well-defined multipole character for nonspherical particles. Finally, it is worth noting that the methodology reported in this work can also be applied to the study of the elastic-field eigenmodes of nonspherical particles<sup>69</sup> and studies of corresponding phononic structures using multiple-scattering techniques,<sup>70–72</sup> by properly extending the analysis presented here to longitudinal field components.

**Acknowledgment.** Financial support by FET-Open project TAILPHOX (Grant Number 233883) is acknowledged.

**Supporting Information Available:** Projection of spherical harmonics onto the  $C_{\infty v}$  and  $D_{\infty h}$  point groups. This material is available free of charge via the Internet at: <http://pubs.acs.org>.

## References and Notes

- Moosmüller, H.; Chakrabarty, R. K.; Arnot, W. P. *J. Quant. Spectrosc. Radiat. Transfer* **2009**, *110*, 844.
- Boisselier, E.; Astruc, D. *Chem. Soc. Rev.* **2009**, *38*, 1759.
- Mie, G. *Ann. Phys. (Leipzig)* **1908**, *25*, 377.
- Debye, P. *Ann. Phys. (Leipzig)* **1909**, *335*, 755.
- Möglich, F. *Ann. Phys. (Leipzig)* **1927**, *83*, 609.
- Bouwcamp, C. J. *Rep. Prog. Phys.* **1954**, *17*, 35.
- Wait, J. R. *Can. J. Phys.* **1955**, *33*, 189.
- Asano, S.; Yamamoto, G. *Appl. Opt.* **1975**, *14*, 29.
- Yang, P.; Liou, K. N. *J. Comput. Phys.* **1998**, *140*, 346.
- Wriedt, T. *Generalized Multipole Techniques for Electromagnetic and Light Scattering*; Elsevier: Amsterdam, 1999.
- Mackowski, D. W. *J. Opt. Soc. Am. A* **2002**, *19*, 881.
- Mishchenko, M. I.; Travis, L. D.; Lacis, A. A. *Scattering, Absorption, and Emission of Light by Small Particles*; Cambridge University Press: Cambridge, 2002.
- Loke, V. L. Y.; Nieminen, T. A.; Parkin, S. J.; Heckenberg, N. R.; Rubinsztein-Dunlop, H. *J. Quant. Spectrosc. Radiat. Transfer* **2007**, *106*, 274.
- Yurkin, M. A.; Hoekstra, A. G. *J. Quant. Spectrosc. Radiat. Transfer* **2007**, *106*, 558.
- Kreibig, U.; Schmitz, B.; Breuer, H. D. *Phys. Rev. B* **1987**, *36*, 5027.
- Ricard, D.; Roussignol, P.; Flytzanis, C. *Opt. Lett.* **1985**, *10*, 511.
- Haus, J. W.; Kalyaniwalla, N.; Inguva, R.; Bowden, C. M. *J. Appl. Phys.* **1989**, *65*, 1420.
- Granqvist, C. G.; Wittwer, V. *Sol. Energy Mater. Sol. Cells* **1998**, *54*, 39.
- Joerger, R.; Gampp, R.; Heinzl, A.; Graf, W.; Köhl, M.; Gantenbein, P.; Oelhafen, P. *Sol. Energy Mater. Sol. Cells* **1998**, *54*, 351.
- Yannopoulos, V. *Phys. Rev. B* **2006**, *73*, 113108.
- Wan, J. T. K.; Chan, C. T. *Appl. Phys. Lett.* **2006**, *89*, 041915.
- Popov, O.; Zilbershtein, A.; Davidov, D. *Appl. Phys. Lett.* **2006**, *89*, 191116.
- Lal, S.; Link, S.; Halas, N. J. *Nat. Photonics* **2007**, *1*, 641.
- Eustis, S.; El-Sayed, M. A. *Chem. Soc. Rev.* **2006**, *35*, 209.
- Khlebtsov, N. G. *Quantum Electron.* **2008**, *38*, 504.
- Bardhan, R.; Grady, N. K.; Cole, J. R.; Joshi, A.; Halas, N. J. *ACS Nano* **2009**, *3* (3), 744.
- Hutter, E.; Pileni, M. P. *J. Phys. Chem. B* **2003**, *107*, 6497.
- Sönnichsen, C.; Franzl, T.; Wilk, T.; von Plessen, G.; Feldmann, J.; Wilson, O.; Mulvaney, P. *Phys. Rev. Lett.* **2002**, *88*, 077402.
- Sherry, L. J.; Chang, S. H.; Schatz, G. C.; Van Duyne, R. P.; Wiley, B. J.; Xia, Y. *Nano Lett.* **2005**, *5*, 2034.
- Zhang, J. Z.; Olson, T. Y. *J. Mater. Sci. Technol.* **2008**, *24* (4), 433.
- Murphy, C. J.; Gole, A. M.; Hunyadi, S. E.; Stone, J. W.; Sisco, P. N.; Alkilany, A.; Kinard, B. E.; Hankins, P. *Chem. Commun.* **2008**, 544.
- Hao, E.; Bailey, R. C.; Schatz, G. C.; Hupp, J. T.; Li, S. *Nano Lett.* **2004**, *4*, 327.
- Wang, Z.; Ma, L. *Coord. Chem. Rev.* **2009**, *253*, 1607.
- Muskens, L. O.; Guillaume, B.; Del Fatti, N.; Vallée, F.; Brioude, A.; Jiang, X.; Pileni, M. P. *J. Phys. Chem. C* **2008**, *112*, 8917.
- Myroshnychenko, V.; Rodríguez-Fernández, J.; Pastoriza-Santos, I.; Funston, A. M.; Novo, C.; Mulvaney, P.; Liz-Marzán, L. M.; García de Abajo, F. J. *Chem. Soc. Rev.* **2008**, *37*, 1792.
- Ohtaka, K. *Phys. Rev. B* **1979**, *19*, 5057.
- Lamb, W.; Wood, D. M.; Ashcroft, N. W. *Phys. Rev. B* **1980**, *21*, 2248.
- Waterman, P. C.; Pedersen, N. E. *J. Appl. Phys.* **1986**, *59*, 2609.
- Stefanou, N.; Modinos, A. *J. Phys.: Condens. Matter* **1991**, *3*, 8135.
- Wang, X.; Zhang, X. G.; Yu, Q.; Harmon, B. N. *Phys. Rev. B* **1993**, *47*, 4161.
- Karathanos, V.; Modinos, A.; Stefanou, N. *J. Phys.: Condens. Matter* **1994**, *6*, 6257.
- Moroz, A. *Phys. Rev. B* **1995**, *51*, 2068.
- Ohtaka, K.; Tanabe, Y. *J. Phys. Soc. Jpn.* **1996**, *65*, 2265.
- Modinos, A.; Stefanou, N.; Yannopoulos, V. *Opt. Express* **2001**, *8*, 197.
- Gantzounis, G.; Stefanou, N. *Phys. Rev. B* **2006**, *73*, 035115.
- Stefanou, N.; Modinos, A. *J. Phys.: Condens. Matter* **1991**, *3*, 8149.
- Ohtaka, K.; Suda, Y.; Nagano, S.; Ueta, T.; Imada, A.; Koda, T.; Bae, J. S.; Mizuno, K.; Yano, S.; Segawa, Y. *Phys. Rev. B* **2000**, *61*, 5267.
- Stefanou, N.; Modinos, A.; Yannopoulos, V. *Solid State Commun.* **2001**, *118*, 69.
- Vincent, P. *Appl. Phys.* **1979**, *18*, 291.
- Brandl, D. W.; Mirin, N. A.; Nordlander, P. *J. Phys. Chem. B* **2006**, *110*, 12302.
- Gantzounis, G.; Stefanou, N.; Papanikolaou, N. *Phys. Rev. B* **2008**, *77*, 035101.
- Khlebtsov, B. N.; Melnikov, A.; Khlebtsov, N. G. *J. Quant. Spectrosc. Radiat. Transfer* **2007**, *107*, 306.
- Ozby, E. *Science* **2006**, *311*, 189.
- García, de Abajo, F. J. *Rev. Mod. Phys.* **2007**, *79*, 1267.
- Kawata, S.; Inoué, Y.; Verma, P. *Nat. Photonics* **2008**, *2*, 438.
- Grigorenko, A. N.; Geim, A. K.; Gleeson, H. F.; Zhang, Y.; Firsov, A. A.; Khrushchev, I. Y.; Petrovic, J. *Nature* **2005**, *438*, 335.
- Soukoulis, C. M.; Linden, S.; Wegener, M. *Science* **2007**, *315*, 47.
- Valentine, J.; Zhang, S.; Zentgraf, T.; Ulin-Avila, E.; Genov, D. A.; Bartal, G.; Zhang, X. *Nature* **2008**, *455*, 376.
- Jackson, J. D. *Classical Electrodynamics*; New York: Wiley, 1999.
- Payne, E. K.; Shuford, K. L.; Park, S.; Schatz, G. C.; Mirkin, C. A. *J. Phys. Chem. B* **2006**, *110*, 2150.
- Khlebtsov, B. N.; Khlebtsov, N. G. *J. Phys. Chem. C* **2007**, *111*, 11516.
- Cornwell, J. F.; *Group Theory in Physics*; Academic: London, 1984; Vol. 1.
- Zhang, F. *Matrix Theory: Basic Results and Techniques*; Springer: New York, 1999.

- (64) Ohtaka, K.; Tanabe, Y. *J. Phys. Soc. Jpn.* **1996**, *65*, 2670.
- (65) Arfken, G. B.; Weber, H. J. *Mathematical Methods for Physicists, International Edition*; Academic Press: New York, 1995.
- (66) Johnson, P. B.; Christy, R. W. *Phys. Rev. B* **1972**, *6*, 4370.
- (67) Purcell, E. M.; Pennypacker, C. R. *Astrophys. J.* **1973**, *186*, 705.
- (68) Draine, B. T.; Flatau, P. J. *J. Opt. Soc. Am. A* **1994**, *11*, 1491.
- (69) Tamura, S. I. *Phys. Rev. B* **2009**, *79*, 054302.
- (70) Sainidou, R.; Stefanou, N.; Modinos, A. *Phys. Rev. B* **2004**, *69*, 064301.
- (71) Sainidou, R.; Stefanou, N.; Psarobas, I. E.; Modinos, A. *Comput. Phys. Commun.* **2005**, *166*, 197.
- (72) Ivansson, S. M. *J. Acoust. Soc. Am.* **2008**, *124*, 1974.

JP908019S